20

LA-3989

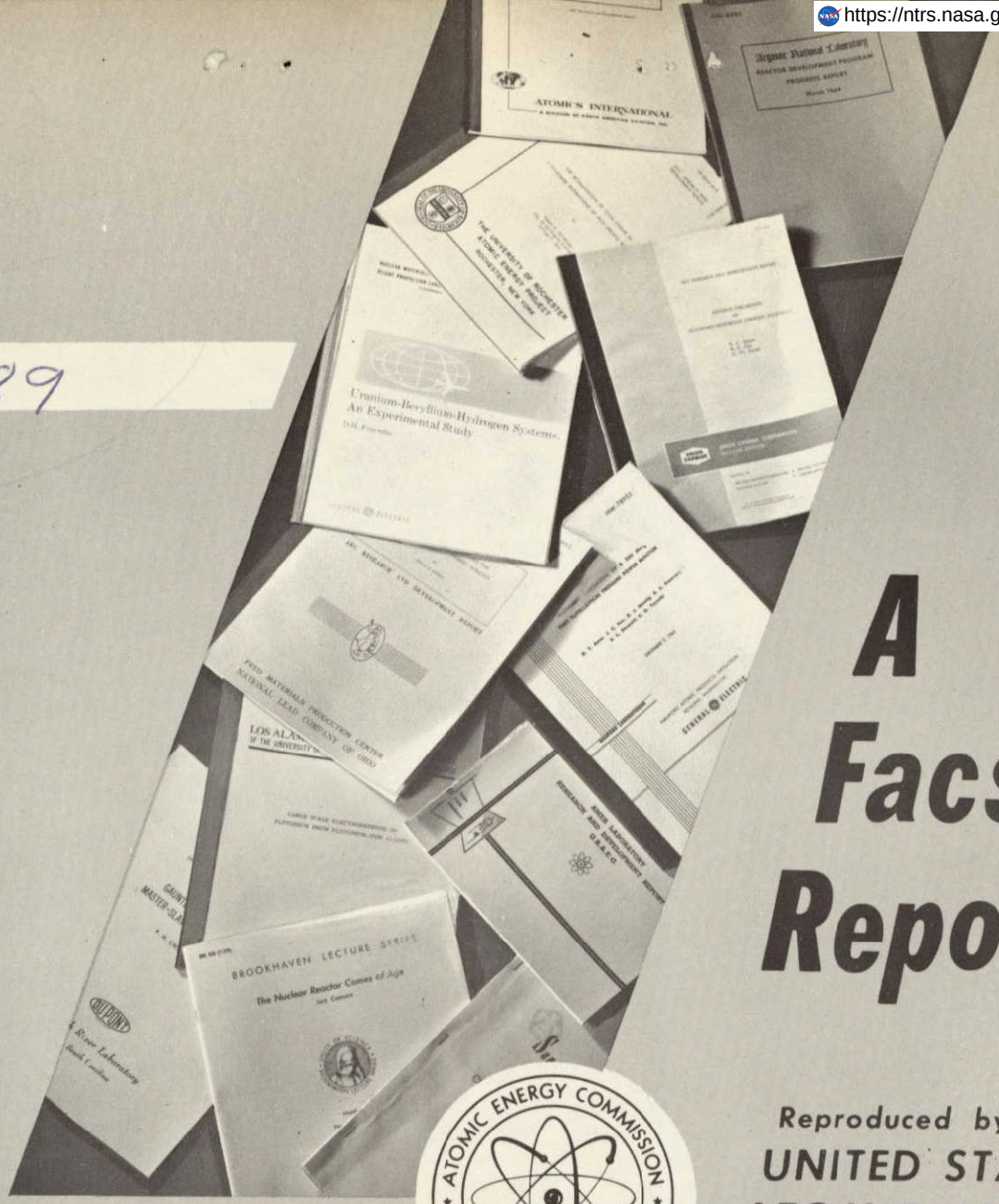

A Facsimile Report

Reproduced by
UNITED STATES
ATOMIC ENERGY COMMISSION
Division of Technical Information
P.O. Box 62 Oak Ridge, Tennessee 37830

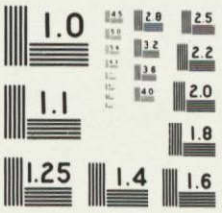

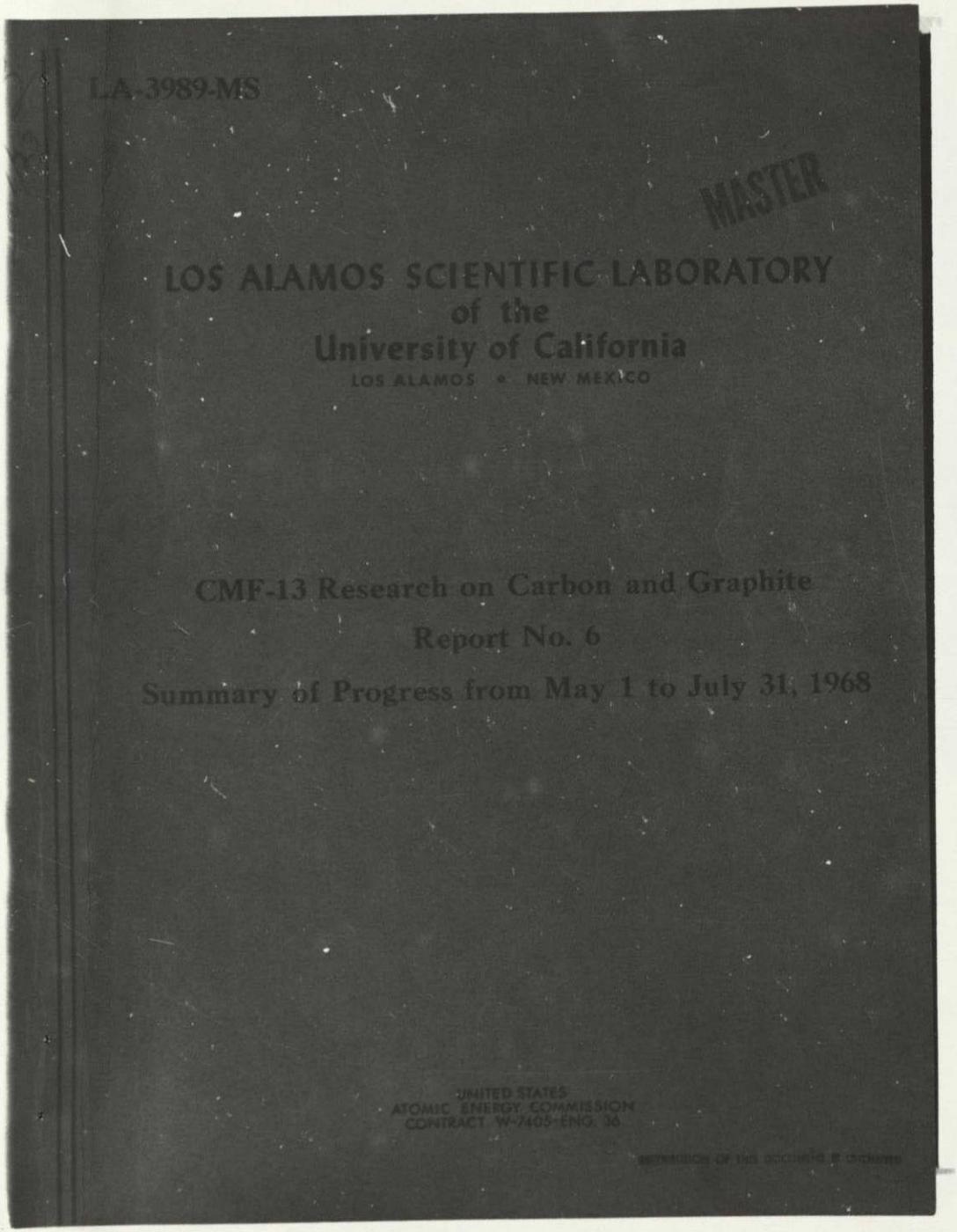
LA-3989-MS
MASTER
LOS ALAMOS SCIENTIFIC LABORATORY
of the
University of California
LOS ALAMOS • NEW MEXICO
CMF-13 Research on Carbon and Graphite
Report No. 6
Summary of Progress from May 1 to July 31, 1968
UNITED STATES
ATOMIC ENERGY COMMISSION
CONTRACT W-7405-ENG. 36

BLANK PAGE

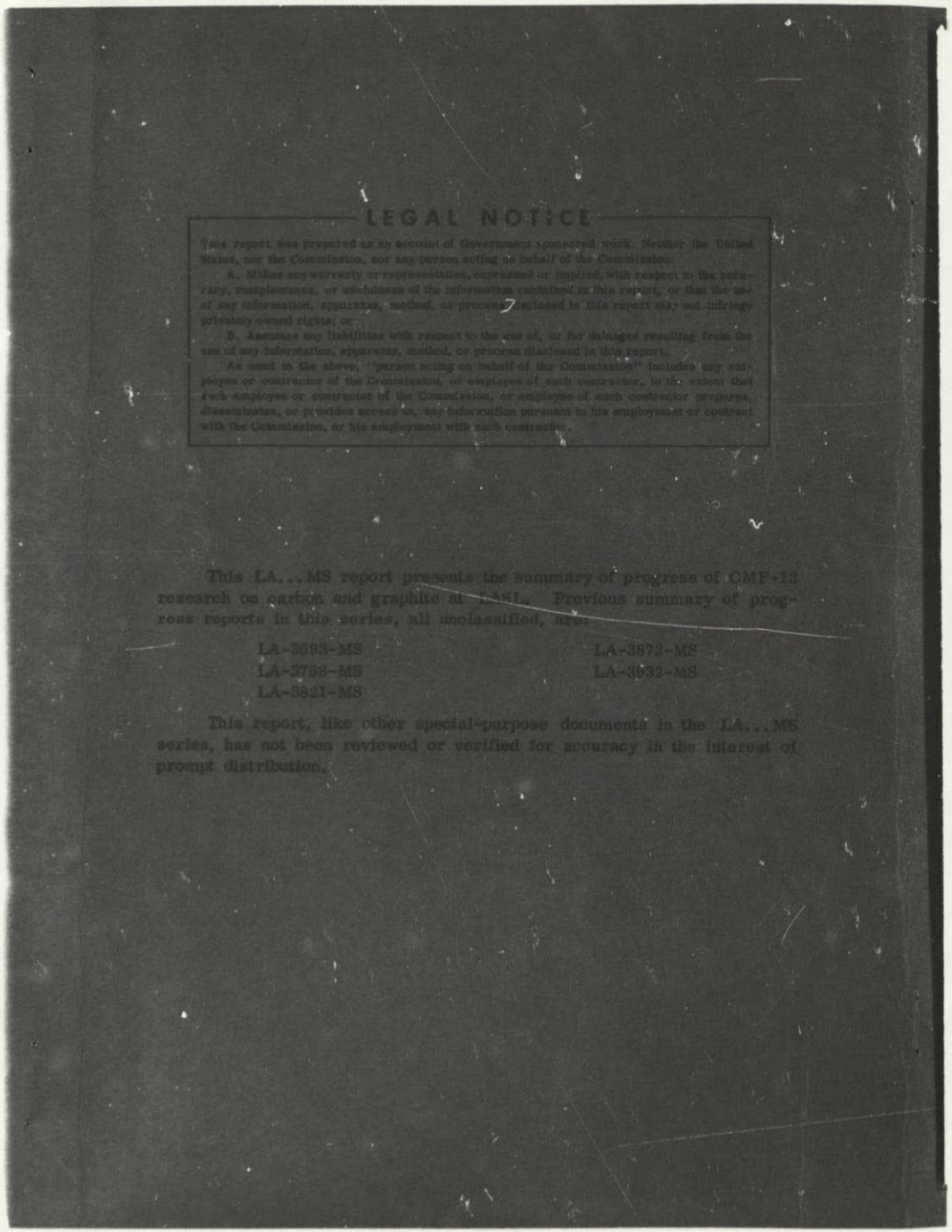

LEGAL NOTICE

This report was prepared as an account of Government sponsored work. Neither the United States, nor the Commission, nor any person acting on behalf of the Commission:

A. Makes any warranty or representation, expressed or implied, with respect to the accuracy, completeness, or usefulness of the information contained in this report, or that the use of any information, apparatus, method, or process disclosed in this report may not infringe privately owned rights; or

B. Assumes any liabilities with respect to the use of, or for damages resulting from the use of any information, apparatus, method, or process disclosed in this report.

As used in the above, "person acting on behalf of the Commission" includes any employee or contractor of the Commission, or employee of such contractor, to the extent that such employee or contractor of the Commission, or employee of such contractor prepares, disseminates, or provides access to, any information pursuant to his employment or contract with the Commission, or his employment with such contractor.

This LA...MS report presents the summary of progress of CMF-13 research on carbon and graphite at [illegible]. Previous summary of progress reports in this series, all unclassified, are:

LA-3693-MS
LA-3758-MS
LA-3821-MS
LA-3872-MS
LA-3932-MS

This report, like other special-purpose documents in the LA...MS series, has not been reviewed or verified for accuracy in the interest of prompt distribution.

BLANK PAGE

LA-3989-MS
SPECIAL DISTRIBUTION

LOS ALAMOS SCIENTIFIC LABORATORY
of the
University of California
LOS ALAMOS • NEW MEXICO

Report distributed September 4, 1968

CMF-13 Research on Carbon and Graphite

Report No. 6

Summary of Progress from May 1 to July 31, 1968*

by

Morton C. Smith

*Supported in part by funds transferred by NASA through the Space Nuclear Propulsion Office.

REPORT NO 6 SUMMARY OF PROGRESS FROM MAY 1 TO JULY 31, 1968

I INTRODUCTION

This is the sixth in a series of progress reports devoted to carbon and graphite research and development in LASL Group CMF-13, and summarizes work done during the months of May June and July, 1968 It should be understood that in such a report many of the data given are preliminary incomplete, and subject to correction and that many of the opinions and conclusions stated are tentative and subject to change This report is intended only to provide up-to-date background information to those who share the interests of the programs described in it, and should not be quoted or used as a reference publicly or in print

Research and development on carbon and graphite were undertaken by CMF-13 primarily to increase understanding of their properties and behavior as engineering materials, to improve the raw materials and processes used in their manufacture, and to learn how to produce them with consistent, predictable, useful combinations of properties The approach taken is microstructural, based on study and characterization of natural, commercial, and experimental carbons and graphites by such techniques as x-ray diffraction, electron and optical microscopy, and porosimetry Physical and mechanical properties are measured as functions of formulation, treatment, and environmental variables, and correlations are sought among properties and structures Raw material and manufacturing techniques are investigated, improved and varied systematically in an effort to create specific internal structures believed to be responsible for desirable combinations of properties Prompt feedback of information among these activities then makes possible progress in all of them toward their common goal of understanding and improving manufactured carbons and graphites

Since its beginning, this program has been sponsored by the Division of Space Nuclear Systems of the United States Atomic Energy Commission, through the Space Nuclear Propulsion Office More recently additional general support for it has been provided by the National Aeronautics and Space Administration, through the Office of Advanced Research and Technology The direct and indirect support and the guidance and encouragement provided by both of these agencies of the United States Government are gratefully acknowledged

II CMF-13 "STATE-OF-THE-ART" GRAPHITE

Lot AAQ1 is a relatively large sample of an extruded, resin-bonded graphite manufactured in CMF-13 primarily to (1) Demonstrate the usefulness of the manufacturing techniques developed by CMF-13 (2) Explore the properties and behavior of a good graphite of this type (3) Provide a base-line against which to compare future graphites in which filler, binder, and manufacturing procedures are varied systematically

The raw materials and manufacture and many of the properties of AAQ1 graphite have been described in previous reports in this series This and additional information collected since the last such report (LA-3932-MS) was written have been summarized in a topical report on AAQ1 graphite now being prepared In anticipation of that report, work recently done on Lot AAQ1 will be reported here only incidentally

III RAW MATERIALS

A Solid Raw Materials (H D Lewis)

1 Small-Particle Statistics

A 7094 computer program FININT has been written for analysis of "size-distribution" data using the finite-interval ('non-functional') model It will be the basic routine for data analysis and mixture calculations for systems which are not well represented by the log-normal ('functional') model and for attempts to synthesize log-normal distributions by mixing non-log-normal systems

The FININT program will handle any number of data sets each consisting of a maximum of 20 subsets, with each subset consisting of data from a maximum of 6 samples or repeat runs on a given material Using volume-fraction weight, or weight-fraction vs 'size' data it computes for each sample the following third-moment statistics weighted mean $\bar{d}_3$ variance $s^2_{d_3}$ skewness, g_{d_3} and coefficient of variation CV_{d_3} The variable size, d, is transformed to $x = \log_e d$ and $\bar{x}3$, s^2_{x3} and g_{x3} are computed Volume-fraction or weight-fraction variates are then transformed to relative frequency and $\bar{d}$ s^2_d, g_d CV_d, $\bar{x}$ s^2_x, g_x and specific surface are calculated Finally the data are pooled for each set and the same statistics calculated as averaged set values The program was written to handle porosimetry as well as particle size data

The COFVARD program, to compute CV_d as a function of composition in mixtures of powders, has also been modified to treat finite-interval data For any desired group of binary combinations of averaged set data from the FININT program it will compute CV_d, CV_{d_3}, s^2_x s^2_d $\bar{d}_3$, $\bar{d}$ and $\bar{x}_3$ at 2 wt % mixture intervals This set of statistics is used in attempt to correlate particle size distributions of filler mixtures with mix behavior in extrusion or pressing and with properties of the finished carbon or graphite

2 Characterization of Cabot Carbon Black

A sample of CMF-13 Lot T-8 carbon black, a thermal black manufactured by Cabot Corporation and identified as Sterling FT grade was dispersed ultrasonically and examined in the electron microscope It consisted of essentially spherical particles, most of which were in the range 0 1 to 0 2μ dia A large proportion of these were aligned in long, twisting, essentially single-file chains, which would be difficult to classify as "agglomerates" An optical particle-size count, made on two electron micrographs at 22,000 X, gave the data and computed sample statistics shown in Fig 1 Because of the difficulty of identifying agglomerates and the relatively small number of particle clusters present which appeared really to be agglomerates, no agglomerate-size count was attempted Mean and most probable particle diameter and variance were all appreciably smaller than for P33 Thermax carbon black which was described in LA-3932-MS

Heat treatment of a small sample of Sterling FT carbon black in a graphite crucible at 2820 C changed the shapes of the particles from spherical to polyhedral, with well-developed facets This is believed to indicate the development of a quite well-graphitized internal structure

B Liquid Raw Materials (E M Wewerka)

1 Stabilities of Furfuryl Alcohol Resins

Some of the experimental furfuryl alcohol resins synthesized in CMF-13 have been observed to increase in viscosity with time Improved methods of neutralizing the polymerization catalyst have increased their stability considerably However some changes in viscosity over the first week of storage are still observed

2 Gel Permeation Chromatography (GPC)

Several new sets of GPC columns have been used to analyze standard resin samples in order to determine the combination of columns most useful for examination of materials of interest here The set finally chosen consists of 5 columns having, in order, maximum pore diameters of 3×10^3, 500, 250, 250, and 60Å Although

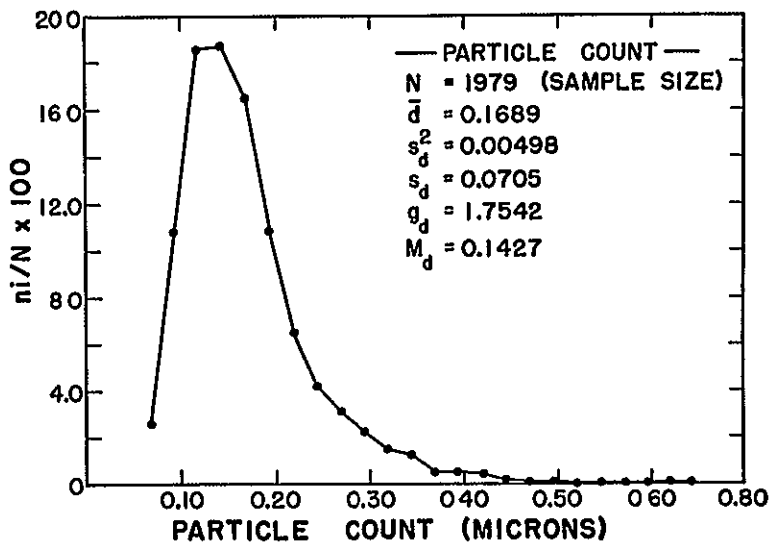

Fig 1 Sample Data and Statistics, Sterling FT Carbon Black, CMF-13 Lot T-8

other combinations of columns gave better resolution of the lower molecular weight species in furfuryl alcohol resins, this set was thought to give better over-all results considering especially the higher molecular weight region

3 Donor-Acceptor Complexes

A study of donor-acceptor complexes has been undertaken The ultraviolet and visible spectra of tetracyanoethylene (TCNE) in methanol, acetonitrile, methylene chloride and acetone have been investigated A number of anomalous effects have been observed with the latter three solvents Spectroscopic data show rapid band changes, indicating that decomposition of the TCNE may be occurring

The spectra of butyl vinyl ether (BVE) have also been investigated in a number of solvents It appears to be relatively stable in solution

A mixture of 10^{-4}M BVE and 10^{-5}M TCNE in methanol gave no spectral evidence of the formation of a donor-acceptor complex The component materials will be carefully purified before this investigation is continued

4 Furfuryl Alcohol-Formaldehyde Copolymers

Two series of furfuryl alcohol-formaldehyde copolymer resins have been synthesized, one with a 2 1 ratio of furfuryl alcohol to formaldehyde and the other with a 1 2 ratio Each series included resins of several different viscosities A few of the resins have been characterized by GPC, gas chromatography and infrared spectroscopy, and a sample of each has been cured baked and graphitized to determine carbon residue and degree of graphitization in the absence of filler

A representative resin from each series has been

TABLE 1

EFFECTS OF REPEATED FLUID ENERGY GRINDING ON SCREEN-SIZE ANALYSIS OF NEEDLE COKE

Grind No	Feed Rate Lb/hr	Cumulative Weight % Coarser Than 710 μ (#25)	350 μ (#45)	177 μ (#80)	88 μ (#170)	41 μ	21 μ	10 μ	5 μ	Fineness % < 5 μ
Raw Feed*	---	6 7	30 0	56 0	79 1	91 7	94 0	96 0	96 8	3 2
T(CN)-1	4 8	1 5	6 0	11 5	23 7	52 7	66 7	78 1	84 5	15 5
-2	4 2	0	0 3	0 8	2 7	11 8	30 7	54 1	70 9	29 1
-3	3 5				0 2	0 9	2 6	24 4	58 6	41 4
-4	3 1				0	trace	trace	9 8	44 1	55 9
-5	2 6					0	0	3 3	34 6	65 4
-6	2 0							0 6	27 0	73 0
-7	2 0							trace	25 3	74 7
-8	2 0							0	23 4	76 6

* CNP-4

mixed with a graphite filler having a large crystallite size and pressed into discs for determination of the degree of graphitization which occurs in the presence of filler The same two resins have been used as binders for the fabrication of extruded rods using the same filler mix and manufacturing conditions used to produce Lot AAQ1 The properties of rods made with the copolymer will be compared directly with those made with Varcum resin.

The lower molecular weight components of several of the copolymer resins have been separated from the bulk by fractional distillation A study of the ability of gas chromatography columns to separate these fractions into pure components has begun If this separation can be made, the components will be analyzed further by infrared spectrometry, nuclear magnetic resonance, or mass spectrometry

IV EXPERIMENTAL GRAPHITE MANUFACTURE

A Grinding Research (R. J Imprescia)

1 Grinding of Commercial Needle Coke

A sample of CMF-13 Lot CNL-1, a lump needle coke purchased from Carbon Products Division of Union Carbide Corporation, was reduced by a series of crushings in a jaw mill and a hammer mill to a particle-size distribution similar to that used in previous fluid-energy fine-grinding experiments In this condition it was identified as Lot CNP-4 This material was then ground in 8 successive passes through the Trost fluid-energy mill the product of the first pass being identified as T(CN)-1, that of the second pass as T(CN)-2, etc Screen analyses of the grinding products are listed in Table 1 Micromerograph analyses in Table 2, and surface area analyses in Table 3 In Table 3, the "S_W Calc " is specific surface area calculated from Micromerograph sample statistics, "S_W BET" is that measured by nitrogen adsorption, and the "Fuzziness Ratio" is the ratio of the two $\bar{d}$ is a mean particle diameter (Stokes effective diameter) calculated from Micromerograph data, and d_s is the calculated diameter of monosized spheres which would have the same specific surface area as that measured by nitrogen adsorption In this series $\bar{d}$ is not a useful sample statistic, apparently because it was calculated using the log-normal approximation for sample distributions which actually were truncated at both extremes The small change in "Fuzziness Ratio" suggests that grinding did not significantly change the surface character of the particles

Specific surface area and relative fineness of the

TABLE 2

SAMPLE STATISTICS FROM MICROMEROGRAPH DATA, GROUND NEEDLE COKE

Sample	μ_{x3}	$\hat{\sigma}_x^2$	μ_x	$\bar{d}_3$ micron	$\bar{d}$ micron	s_d^2 micron^2	CV_d
T(CN)-1	3 5062	1 7409	-1 7165	79 574	0 429	0 866	2 169
T(CN)-2	2 5507	1 1020	-0 7555	22 237	0 815	1 336	1 418
T(CN)-3	1 9313	0 56612	0 23291	9 156	1 675	2 137	0 873
T(CN)-4	1 6804	0 4490	0 3334	6 719	1 747	1 730	0 752
T(CN)-5	1 6005	0 40581	0 3826	6 068	1 796	1 6143	0 708
T(CN)-6	1 5103	0 3975	0 3178	5 524	1 676	1 371	0 699
T(CN)-7	1 4895	0 4039	0 2779	5 428	1 616	1 299	0 705
T(CN)-8	1 4940	0 3834	0 3421	5 398	1 706	1 302	0 684

TABLE 3

SURFACE AREA SAMPLE STATISTICS, GROUND NEEDLE COKE

Sample	S_W, m^2/g Calc	S_W, m^2/g BET	$\bar{d}$ micron	d_s micron	"Fuzziness Ratio" R_F
T(CN)-1	0 203	5 29	0 429	0 535	26 10
T(CN)-2	0 383	10 81	0 815	0 262	28 22
T(CN)-3	0 545	18 90	1 675	0 150	34 67
T(CN)-4	0 660	22 56	1 747	0 125	34 18
T(CN)-5	0 700	23 67	1 796	0 120	33 81
T(CN)-7	0 781	24 79	1 616	0 114	31 74
T(CN)-8	0 770	25 81	1 706	0 110	33 51

needle coke are plotted in Fig 2 as functions of number of passes through the fluid-energy mill The grinding behavior is generally similar to that of several other raw materials previously investigated, but with some interesting differences Thus, in Fig 3, relative fineness vs number of grinding passes is plotted for the T(Na) series of natural graphite flours, the T(YBF) series of commercial polycrystalline graphites, and the T(HCTE) series of high-expansion cokes as well as for T(CN) needle coke Initially the needle coke grinds more easily than either the commercial graphite or the high-expansion coke However, after a few passes through the mill it becomes much more difficult than the commercial graphite to grind further, and may be approaching a degree of difficulty similar to that of the high-expansion coke

Table 2 shows monotonic decreases in μ_{x3} and $\bar{d}_3$ for successive passes of the needle coke through the mill, and a rapid decrease in $\hat{\sigma}_x^2$ through the first three passes This behavior is different from that of either the commercial graphite or the high-expansion coke, which have been discussed in earlier reports in this series (LA-3821-MS, LA-3872-MS and LA-3932-MS)

Crystalline parameters of the grinding feed and of several of the ground products were measured by x-ray diffraction and are listed in Table 4 No significant change in crystallite size L_c, and no measurable change in interplanar spacing d_{002}, were produced by grinding

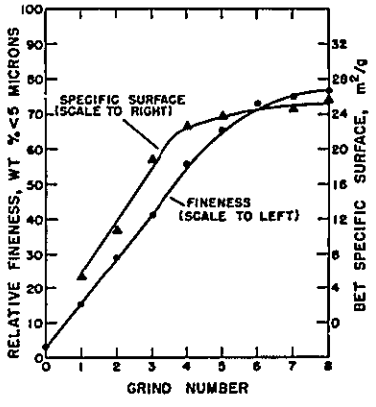

Fig 2 Relative Fineness and Specific Surface Area of Needle Coke Series T(CN) as Functions of Number of Fluid-Energy Grinding Passes

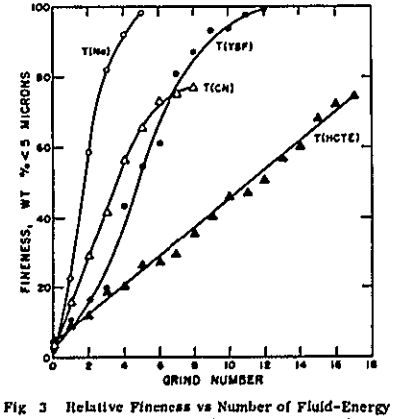

Fig 3 Relative Fineness vs Number of Fluid-Energy Grinding Passes for Four Different Raw Materials

TABLE 4

CRYSTALLINE PARAMETERS

OF TROST-MILLED NEEDLE COKE

Sample Designation	L_c (A)	d_{002} (A)
CNP-4	41 3	3 44
T(CN)-1	41 3	3 44
T(CN)-2	40 6	3 44
T(CN)-4	39 9	3 44
T(CN)-6	40 2	3 44
T(CN)-8	39 3	3 44

the needle coke

The grinding feed and several of the ground products were also examined by both optical and electron microscopy The feed material, Lot CNP-4, had the typical microstructure expected of a needle coke with relatively long straight sections of 'grain" The larger particles contained many internal voids of the cleavage fracture type Typically these were long and straight, and frequently they occurred in parallel sets During grinding fracture occurred preferentially through such voids, producing acicular smaller particles As a result there was a progressive reduction in void content and a progressive increase in particle acicularity as grinding continued Particles under about 50μ dia had little internal porosity and were much more acicular than were coarser particles, and particles finer than about 20μ dia were extremely acicular

2 Hot Molding of Grinding Products

As one means of evaluating the products of the grinding studies described above, a series of these products have been used as fillers to produce hot-molded, pitch-bonded graphite discs The binder used in all cases was Allied Chemical Co Grade 30MH coal-tar pitch (CMF-13 Lot No PP-3), in the concentration determined by the lubricant-evaporation technique to be optimum for each material The mixes were compacted in 2 5-in dia graphite dies at 4000 psi, which was maintained during

TABLE 5

PROPERTIES OF HOT-MOLDED, PITCH-BONDED GRINDING PRODUCTS

Specimen No	Filler Used	Filler Fineness % <6 μ	Bulk Density, g/cm³ Baked	Bulk Density, g/cm³ Graph	% Vol Change Baked to Graph	Young's Modulus 10^6 psi‡	Compressive Strength psi‡	Crystalline Anisotropies σ_{oz}/σ_{ox}	Crystalline Anisotropies M
35 A	CP(HCTE)-2*	4 7	1 487	1 695	-16 7	0 92	7 645	1 00-1 02	<0 1
B	T(HCTE)-1	9 3	1 560	1 825	-17 7	1 19	12,166	1 00-1 01	<0 1
C	T(HCTE)-6	27 0	1 570	1 883	-20 1	---	20,804	1 00-1 02	<0 1 Cracked
D	T(HCTE)-11	46 7	1 544	1 844	-20 4	1 82	---	1 09	0 71 Cracked
E	T(HCTE)-14	60 2	1 557	1 859	-20 4	---	---	1 21	1 02 Cracked
F	T(HCTE)-17	74 1	1 554	1 847	-19 9	1 81	21,578	1 15	0 87 Cracked
36 A	CNP-4*	3 2	1 695	1 626	+2 8	0 46	1,478	1 81	2 8
B	T(CN)-1	16 5	1 742	1 731	-0 8	1 14	3,620	1 84	3 0
C	T(CN)-2	20 1	1 714	1 746	-3 2	1 67	6,310	2 39	4 8
D	T(CN)-3	41 4	1 696	1 760	-5 1	2 28	7,603	3 30	6 5
F	T(CN)-5	65 4	1 686	1 763	-5 7	2 68	7,757	3 64	7 5 Cracked
I	T(CN)-8	76 6	1 691	1 773	-6 0	2 84	9 951	3 83	8 1
37 A	GP(Na)-8*	2 3	2 072	1 952	+4 4	1 02	1,531	2 02	3 2
B	T(Na)-1	22 6	1 964	1 897	+2 1	1 20	6,807	3 45	7 0
C	T(Na)-2	58 6	1 943	1 889	+1 4	3 05	8,209	3 55	7 6
D	T(Na)-3	82 1	1 924	1 874	+1 1	3 23	9,083	3 67	7 2
E	T(Na)-4	92 0	919	1 872	+1 0	3 23	9 454	3 45	7 2
F	T(Na)-5	98 2	1 904	1 850	+1 3	3 27	9,827	3 37	7 1
39 A	GP(Py)-2*	1 7	1 901	1 777	+6 8	---	---	---	---Delaminated
B	T(Py)-1	11 7	1 910	1 903	0 0	2 55	5,954	7 1	10 2
C	T(Py)-3	32 2	1 894	1 904	-0 9	2 53	8 334	6 4	8 7
D	T(Py)-4	35 1	1 898	1 903	-0 7	2 36	8 592	7 4	7 9

* Feed material for fluid-energy grinding

‡ Properties measured normal to molding force (with grain)

a 6 hr heating cycle to 900°C The compacted discs were between 5/8 and 3/4 in thick, and in all cases the binder-residue values for the hot-molded (baked) specimens indicated that at least a sufficient amount of binder had been used The discs were graphitized in flowing helium for 30 min at approximately 2800 C Their densities, shrinkage behavior, and some of their properties are listed in Table 5 Data are reported for the T(HCTE) series of ground high-expansion cokes, the T(CN) series of needle coke flours the T(Na) series of natural graphites, and the T(Py) series of pyrolytic graphites

a T(HCTE) Fillers (35 Series)

The fillers used in this series were a crushed, isotropic air-blown coke ("Robinson coke") having a high coefficient of thermal expansion and the products of grinding it in 1, 6, 11, 14 and 17 passes through the Trost fluid-energy mill The particles in all cases were blocky and approximately equiaxed although perhaps less nearly so in the finest sizes observable by electron microscopy

Except for the first member of the series which was made from the comparatively coarse grinding feed and had relatively low density, both baked and graphitized densities were nearly constant in spite of increasing fineness of the filler Shrinkage during graphitizing was high in all cases, presumably because the coke had been calcined only to about 850°C by its manufacturer All but the first two members of the series cracked severely in a radial pattern during hot molding usually producing pie-shaped fragments The first three members of the series were essentially isotropic Both elastic modulus and strength increased rapidly with increasing filler fineness early in the series and very high compressive strengths were attained

Specimen 35A made from the grinding feed, was observed microscopically to contain many angular pores and numerous long thin gaps between particles, apparently formed by extensive inhomogeneous contraction at some stage of heat treatment With progressively finer filler materials pores became smaller and more nearly equiaxed and the structure was less well penetrated by the mounting resin In the three specimens made from the finest fillers a few lenticular volumes of undistributed binder residue were observed indicating existence of a mixing problem Mixing was apparently good in the first three members of the series but here there appeared to have been insufficient fine filler to fill the voids between the coarser particles

b T(CN) Fillers (36 Series)

For this series of hot-molded specimens the fillers used were the ground needle cokes described above Baked densities showed no clear trend, but both graphitized density and shrinkage during graphitization increased continuously with increasing fineness of the filler Increasing particle acicularity in the finer sizes was reflected in increasing anisotropy, which was very high in the later members of the series The combination of increasing density increasing anisotropy, and probably other factors, caused with-grain elastic modulus and compressive strength to increase continuously with filler fineness All specimens were sound except No 36F, which broke into two nearly equal pieces during molding, and did so again when the run was repeated

Microscopically, the early members of the series were observed to contain large numbers of large pores, appeared to be deficient in binder and showed some evidence of incomplete mixing With finer fillers the number and size of pores decreased and the last three members of the series were not well impregnated by the mounting resin In the last four specimens in the series the filler particles were very acicular in section, with a high degree of alignment parallel to the die walls near the cylindrical surface and parallel to the punch face elsewhere

c T(Na) Fillers (37 Series)

The T(Na) fillers used to produce Series 37 graphite specimens were natural graphite flours ground in the Trost fluid-energy mill In all sizes, the particles composing these flours were very acicular and somewhat shredded in appearance with the lamellar or scaly internal structures typical of a well-graphitized material

All members of this series expanded during graphitization, the expansion being greatest for specimens made from the coarsest fillers Densities in both the baked and the graphitized conditions were high but decreased with increasing fineness of the filler Anisotropy was high, and increased sharply with the first reduction in filler-particle size With-grain elastic modulus and compressive strength increased continuously throughout the series in spite of decreasing bulk density and -- in later members of the series -- nearly constant anisotropy

Specimen 37A made from the relatively coarse grinding feed contained many long, narrow pores oriented with their long axes parallel to the grain These were probably responsible for the fact that, in spite of very high density, the elastic modulus and compressive strength of this graphite were low Specimens made with finer fillers were less well penetrated by the mounting resin so that the void structure was not delineated Evidently, however in spite of continuously decreasing density, the use of progressively finer fillers reduced the degree of interconnectedness of the voids, and the isolated voids which remained were progressively less damaging to mechanical properties

d T(Py) Fillers (39 Series)

Series 39 of hot-molded graphites contained as fillers a series of ground pyrolytic graphite flours Due to easy cleavage of the layered pyrographite structure during crushing and grinding, these were the most acicular flours so far examined Preferred orientation and anisotropy of specimens made from them were correspondingly high

The first member of this series, made from the coarsest filler, expanded considerably during graphitization This expansion was produced by extensive delamination of the larger pyrographite filler particles, which created large intraparticle voids and relatively low specimen density Subsequent specimens, made from progressively finer fillers, showed very little volume change during graphitizing, but in fact were observed to shrink significantly in the across-grain direction (disc thickness) and expand by an equivalent amount in with-grain directions (disc diameters) With the finer fillers bulk densities were high, penetration of the mounting resin was poor, and the void structure was not delineated for microscopic study Evidently, however, little or no delamination occurred, and the voids which remained were not extensively interconnected

B Evaluation of Commercial Fillers (R J Impresario)

As part of a raw-materials evaluation program, hot-molded graphite specimens (Series 34) have been prepared from 26 commercial filler materials now on hand in CMF-13, and are being evaluated with regard to structure and properties The binder used in all cases has been Allied Chemical Co Grade 30MH coal-tar pitch (CMF-13 Lot No PP-3), in the amounts determined to be optimum for each filler by the lubricant-evaporation technique The pitch was ground to approximately 50% minus 200 mesh and blended with the filler in a 2-qt twin-shell blender, using the intensifier in the case of the finer filler materials but -- to avoid comminution -- not using it for the coarser ones The mixes were hot-molded in 2 5-in dia graphite dies at 900°C and 4000 psi, then graphitized for 30 min in flowing helium at 2850°C Filler materials, fabrication characteristics, and some of the properties of the graphites produced are listed in Table 6 Additional properties are listed in Table 7 and microstructures are described briefly in Table 8 (Many of the fillers used have been described individually in previous reports in this series)

The binder residue values listed in Table 6 are generally low, indicating loss of binder by squeeze-out in the die Usually this is taken to indicate that too much binder was used However microscopic observations of binder-deficient areas in many of the specimens suggest instead that the real problem was that of incomplete mixing

With only one exception (Carbon Products' needle coke) the use of coke fillers resulted in volume shrinkage during graphitization The amount of shrinkage varied widely, but was extremely high for the finer Gilsocarbons With two exceptions, the use of graphite fillers resulted in volume expansion during graphitization, the typical expansion being 2 to 4%. The high-CTE graphites were exceptional in this regard

In the microscopic study of these hot-molded graphites, it was apparent that the use of coarse flours containing insufficient fines produced porous graphites usually containing many large pores and large shrinkage breaks between filler particles and binder The degree to which this can be overcome by fine additions to such fillers will be investigated

Microscopically, the best graphites in the series appeared to be 34N S, T and U All of these contained

TABLE 6

FILLER MATERIALS, DENSITIES, SHRINKAGES AND BINDER RESIDUES,

HOT-MOLDED GRAPHITES, SERIES 34

Graphite No	Filler: CMF-13 Lot No	Filler: Manufacturer *	Filler: Type **	Pitch Binder, pph	Density, g/cm³: Baked FPP ‡	Density, g/cm³: Baked Bulk	Density, g/cm³: Graphitized FPP ‡	Density, g/cm³: Graphitized Bulk	Binder Residue %	% Vol Change, Baked to Graph
34A	C-1	GL	80M Coke	33	1 321	1 478	1 373	1 479	37 2	-3 8
B	C-3	AG	100M Gilsocarbon	30	1 513	1 686	1 601	1 694	38 1	-5 5
C	C-4	AG	200M Gilsocarbon	32	1 431	1 642	1 625	1 779	45 9	-11 9
D	C-5	AG	325M Gilsocarbon	32	1 431	1 659	1 623	1 797	49 7	-11 8
E	C-6	GL	3020 Coke	35	1 429	1 637	1 552	1 722	41 6	-7 9
F	C-7	GL	3011 Coke	37	1 448	1 655	1 555	1 721	38 5	-6 9
G	C-8	GL	3009 Coke	28	1 495	1 675	1 576	1 709	42 8	-5 1
H	C-9	GL	3017 Coke	32	1 363	1 521	1 386	1 494	36 3	-1 7
I	C-10	GL	3007 Coke	30	1 368	1 499	1 382	1 461	31 9	-1 0
J	C-11	GL	3021 Coke	37	1 330	1 498	1 363	1 484	34 1	-2 5
K	C-12	GL	3008 Coke	35	1 341	1 513	1 369	1 492	36 7	-2 0
L	CN-3	CP	Needle Coke	28	1 547	1 690	1 535	1 641	33 1	+0 8
M	CNN-1	CP	Non-needle Coke	28	1 520	1 668	1 539	1 646	34 9	-1 3
N	G-12	GL	1008 Graphite	23	1 736	1 891	1 692	1 837	38 8	+3 4
O	G-14	CP	GP BB4 Graphite	27	1 684	1 835	1 624	1 744	33 3	-3 7
P	G-15	CP	GP BB5 Graphite	28	1 659	1 803	1 606	1 725	30 9	+3 3
Q	G-16	GL	1011 Graphite	27	1 680	1 830	1 617	1 753	33 0	+3 9
R	G-17	GL	1012 Graphite	33	1 636	1 808	1 586	1 744	31 7	+3 2
S	G-18	GL	1008 Graphite (M3)	23	1 730	1 878	1 686	1 822	37 1	+2 6
T	G-19	CP	GP48 Graphite	22	1 729	1 908	1 690	1 858	47 0	+2 4
U	G-20	CP	GP38 Graphite	22	1 733	1 910	1 696	1 862	46 6	+2 2
V	G-21	SW	1651 Natural Graph	27	1 728	1 940	1 701	1 847	45 5	+1 6
W	G-22	SW	1652 Natural Graph	20	1 865	1 994	1 819	1 862	38 4	+2 5
X	G-23	CP	HCTE ## Graphite	30	1 601	1 775	1 599	1 764	36 2	+0 2
Y	G-24	CP	HCTE ## Graphite	33	1 507	1 771	1 592	1 784	38 7	-1 4
Z	G-25	CP	HCTE ## Graphite	30	1 608	1 776	1 600	1 758	34 8	+0 5

* Manufacturer GL = Great Lakes Carbon Corporation CP = Carbon Products Div Union Carbide Corp

AG = American Gilsonite Company

SW = Southwestern Graphite Company

‡ FPP = filler-particle packed density

** M = mesh (screen-size)

HCTE = high coefficient of thermal expansion (air-blown isotropic)

TABLE 7

PROPERTIES OF HOT-MOLDED GRAPHITES, SERIES 34

Lot No	Young's Modulus 10^6 psi *	Compr Strength psi *	Electrical Resistivity μΩ cm: * wg	Electrical Resistivity μΩ cm: ** ag	Thermal Conductivity w/cm-C: * wg	Thermal Conductivity w/cm-C: ** ag	Thermal Exp Coeff Ave 25-645°C, x10^{-6}/°C: * wg	Thermal Exp Coeff Ave 25-645°C, x10^{-6}/°C: ** ag	Anisotropy: Crystallite M	Anisotropy: σ_{oz}/σ_{ox}	Anisotropy: Electr Resist	Anisotropy: Thermal Cond	Anisotropy: Thermal Exp
34A	0 37	1 759	2041	---	0 46	0 47	4 75	6 52	0 55	1 07	---	0 98	1 37
B	1 21	6 987	1285	1999	1 08	0 86	4 81	7 17	1 34	1 24	1 56	1 26	1 49
C	1 42	12,529	1240	1628	1 12	0 82	5 79	7 16	1 03	1 26	1 31	1 37	1 24
D	1 53	13 750	1245	1739	1 04	0 74	5 74	7 49	1 16	1 22	1 40	1 41	1 30
E	1 31	8,322	1020	1837	1 30	0 80	4 41	8 00	1 85	1 42	1 80	1 63	1 81
F	1 27	8,007	1034	1874	1 30	0 78	4 45	7 09	1 25	1 37	1 81	1 67	1 59
G	1 03	6,018	1018	1549	1 29	0 86	4 51	6 70	1 24	1 25	1 52	1 50	1 49
H	0 32	1,467	2409	---	---	---	4 00	5 76	---	---	---	---	1 44
I	---	1,069	---	2413	---	---	4 50	4 90	0 3	1 05	---	---	1 09
J	0 39	1 531	1767	2754	---	0 50	3 60	6 26	1 01	1 16	1 56	---	1 74
K	0 35	1,377	2131	2948	0 60	0 50	4 26	5 98	---	---	1 38	1 20	1 40
L	0 86	2,805	1025	3354	0 77	0 42	2 72	7 74	3 4	1 67	3 27	1 83	2 85
M	0 90	3,455	1060	2025	0 74	0 53	3 47	6 67	1 40	2 83	1 91	1 40	1 92
N	1 24	7,456	1013	1549	0 90	0 74	4 01	6 77	1 46	1 189	1 53	1 22	1 69
O	0 91	4,072	1087	1887	0 84	0 72	3 69	6 58	~1 14	~1 25	1 74	1 17	1 78
P	0 80	3,595	1165	1999	0 83	0 70	4 01	7 45	~1 24	~1 52	1 72	1 19	1 86
Q	0 84	3 350	1022	2109	0 85	0 67	3 85	7 36	2 1	~1 42	2 06	1 27	1 91
R	0 86	4,140	1056	2008	0 94	0 71	4 07	7 40	2 1	1 29	1 90	1 32	1 82
S	1 37	6,044	945	2093	0 93	0 70	4 04	8 23	2 51	1 58	2 21	1 33	2 04
T	1 76	7,330	933	2823	1 02	0 49	3 22	8 89	3 10	1 68	3 03	2 08	2 76
U	3 84	6,570	502	3887	0 94	0 41	---	11 09	3 50	3 39	7 74	2 29	---
V	2 31	6,784	817	6824	1 19	0 21	2 14	16 82	10 0	5 44	8 35	5 67	7 39
W	3 49	4,361	438	6761	1 13	0 28	---	17 68	11 1	4 99	15 44	4 04	---
X	1 24	10,632	1506	1611	0 74	0 76	7 12	7 27	0 25	1 029	1 07	0 97	1 02
Y	1 37	13,688	1607	1778	0 69	0 70	5 87	7 63	0 20	1 013	1 11	0 99	1 30
Z	1 24	10,516	1480	1679	0 75	0 75	7 11	7 81	0 26	1 030	1 13	1 00	1 10

* With-grain orientation

** Across-grain orientation

TABLE 8

ELECTRON AND OPTICAL MICROSTRUCTURES OF HOT-MOLDED GRAPHITES, SERIES 34

Graphite No	Microstructure
34A	Many large pores and c-face cracks Too few fines for good packing Mixing inadequate
34B	A few large pores, many colonies of small and medium-sized ones Pores interconnected Mixing doubtful Some large lamellar particles
34C	No large pores or large lamellar particles Colonies of small and medium-sized voids, well connected
34D	Mounting resin penetrated only 300μ surface layer, so voids not delineated Looked sound well mixed
34E	Many long thin voids oriented with grain structure and many colonies of small voids Pores interconnected Preferred orientation evident
34F	Many of the large filler particles outlined by small voids A few large c-face cracks Pores interconnected Mixing doubtful
34G	Many voids of all sizes and shapes, including coarse ones Many long, thin c-face cracks Many fines appear to float freely in voids Both binder and mixing may have been insufficient
34H	Similar to 34G but with more very large pores and broken binder bridges in large binder areas
34I	Very large cracks throughout Binder bridges usually pulled loose at one end or ruptured in binder residue Much interconnected porosity including intraparticle voids not filled by binder Mixing inadequate and may have lacked binder
34J	Similar to 34I Much void space
34K	Similar to 34I and 34J
34L	Closer packing of filler particles than 34I, J, and K Particles very flaky with evident preferred orientation Many cracks and intraparticle voids Appeared binder deficient
34M	Many large voids colonies of voids and c-face cracks, although appeared less porous than 34L Probably binder deficient
34N	Mounting resin penetrated only 600μ surface layer Particle size distribution looked good for packing Structure appeared dense and tight Some small void colonies and intraparticle voids
34O	A few large voids and colonies of voids generally interconnected Insufficient binder or mixing or both
34P	Similar to 34O but more large voids Particle size distribution appeared poor for packing
34Q	Similar to 34P
34R	Similar to 34P Coarse open pore network
34S	Mounting resin penetrated only 500μ surface layer Small void colonies, c-face cracks, and intraparticle voids observed but porosity low pore network tight, and fine particles well packed in voids
34T	Mounting resin penetrated only about 350μ Like 34S but denser appearance and obvious preferred orientation Appears deficient in fines
34U	Very little penetration by mounting resin Similar to 34S and 34T but a still tighter, less porous structure Strong preferred orientation
34V	Very little penetration by mounting resin Little porosity except in association with lenticular pockets of binder residue Very strong preferred orientation Electron microscope showed many fine inclusions with metallic appearance
34W	Very similar to 34V
34X	Many voids in a variety of sizes and shapes, in general more nearly equiaxed than with standard coke

TABLE 8 (Continued)

Graphite No	Microstructure
	fillers and well interconnected Filler particles have internal structures typical of HCTE coke Interparticle bonds look sound interfaces frequently invisible Structure of binder residue much like that of filler, so binder distribution not usually observable Occasional particles of conventional coke in structure No c-face cracks observed
34Y	Mounting resin penetrated only about 1000μ Similar to 34X but with smaller filler particles, smaller voids
34Z	Similar to 34X except slightly finer pore system, fewer large voids Pores interconnected

graphite flour fillers and had good properties, but all were relatively anisotropic

C Mixing Experiments

1 The G-20/G-17 Binary Series (R J Impresciа)

Mixtures of two graphite flours, CMF-13 Lots G-20 and G-17 have been examined for particle-packing behavior using the same blending, filler lubrication, and pressing procedures described in previous reports in this series Results are plotted in Fig 4, where each

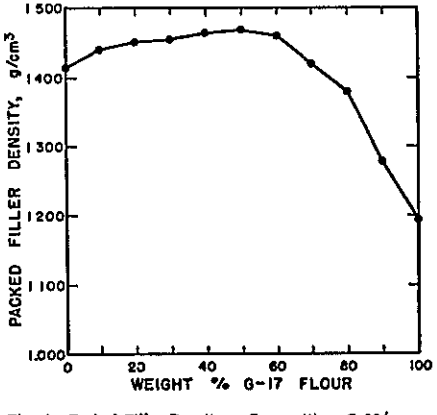

Fig 4 Packed Filler Density vs Composition, G-20/G-17 Binary Mixtures

represents the average of two independent results -- which in every case agreed almost exactly For this system, maximization both of variance and of coefficient of variation indicated that maximum packing density should occur for a mixture containing approximately 98% G-17 flour In fact, the experimental results show a low, broad maximum at about 50% of each component

2 G-18/G-24 and G-18/G-25 Combinations (J M Dickinson)

Because of the interesting properties of the HCTE graphite flours, CMF-13 Lots G-24 and G-25, an attempt has been made to modify their fabrication behavior by adding to them a well-behaved normal graphite flour, CMF-13 Lot G-18 The compositions, manufacturing conditions, and properties of the extruded Series ABB graphites so far made in this attempt are summarized in Tables 9 and 10 In all cases 15 parts of regular Thermax carbon black were added to the mix, from either of two presumably identical lots The binder used throughout was Varcum, a commercial furfuryl alcohol resin

The addition of G-18 flour had the desired effect of preventing the severe cracking which occurred during graphitization of extruded lots made from HCTE flours alone So far as they have been determined to this point, the properties produced by the flour mixtures are intermediate between those produced by the unmixed flours Graphite ABB2, containing equal quantities of HCTE and

TABLE 9

COMPOSITIONS AND EXTRUSION CONDITIONS ABB GRAPHITES

Specimen No	Composition: HCTE Flour, Parts	G-18 Flour Parts	Thermax, Parts	Binder pph	Extrusion Conditions: Pressure, psi	Speed, in /m in	Temp , °C
AAP27	85 G-24	---	15 TP-3	28 4	7600	167	50
ABB2	42 5 G-24	42 5	15, TP-4	27	7300	116	52
ABB3	21 25 G-24	63 75	15 TP-4	27	6400	150	55
AAP24	85, G-25	---	15 TP-3	23 95	3800	171	45
ABB1	42 5 G-25	42 5	15, TP-4	24	7300	112	48
AAP30	---	85	15 TP-4	27	7600	171	47

TABLE 10

PROPERTIES OF AAB GRAPHITES

Specimen No	Green Dia in	Density, g/cm^3	Electrical Resistivity, μ Ω cm	Young's Modulus,* 10^6 psi	Carbon Residue, %	Inspection
AAP27	0 5015	1 910±0 01	1915±59	1 96	49 8±0 3	Cracked on graph
ABB2	0 5035	1 911±0 003	1258±33	2 13±0 02	48 3±0 3	OK
ABB3	0 504	1 890±0 003	1152±29	2 27±0 02	47 1±0 4	OK
AAP24	0 4995	1 913±0 002	1737±10	1 95±0 01	50 6±0 3	Cracked on graph
ABB1	0 502	1 892±0 003	1270±25	1 99±0 02	47 5±0 5	OK
AAP30	0 5015	1 880±0 002	986±44	2 47±0 02	47 1±0 4	OK

* With-grain

normal flours, is especially interesting in having the high density typical of the HCTE materials a relatively high elastic modulus, and relatively low electrical resistivity

3 Other Binary Combinations (R J Impresciа)

Some of the Series 34 graphites listed in Table 8 have anisotropies lower than any previously observed in CMF-13 experimental graphites Their densities, however are relatively low, and their permeabilities are undoubtedly high In every case they were made without additions of carbon black or any other fine filler component and it is evident that in no case was the size distribution of the filler used ideal for close packing of filler particles

In the hope of developing a nearly isotropic, low-permeability graphite made from commercially available materials, a group of the fillers listed in Table 6 has been selected for mixing experiments This includes 3 coarse fillers (C-1, C-10 and G-14) and 3 fine fillers (C-3, C-8 and G-24) Of these, 4 (identified by the letter C) are coke flours and 2 are graphite flours Eight binary combinations of these, each consisting of one coarse and one fine component, are being examined These are

C-1/C-3	C-8/C-3
C-1/G-24	C-8/G-24
C-10/C-3	G-14/C-3
C-10/G-24	G-14/G-24

Because of the danger of comminution of the coarse fractions during intensive mixing, the fillers are blended together in a Fisher-Kendall laboratory bottle blender, which has a very gentle mixing action After blending the dry mix for 10 min an amount of stearic acid lubricant somewhat less than the optimum is added and blending is continued for another 10 min The mixture is then compacted in a 1 5-in dia steel die at the relatively low pressure of about 900 psi -- again to avoid crushing of particles From the known weight of filler and the dimensions of the compacted mixture a packed filler density is calculated

When filler combinations are found which pack well they will be used to produce hot-molded, pitch-bonded graphites whose properties will be compared with those of similar graphites containing only one filler component The addition of carbon blacks will then be considered

D The Role of Carbon Black in Graphite (J M Dickinson)

In the last previous report in this series (LA-3932-MS), an investigation was described which is intended to shed light on the behavior and effects of carbon black when it is used as a component of the filler mix in the manufacture of carbons and graphites In the first phase of this program, volume changes of the dry filler are observed as it is compressed in an evacuated steel die unloaded, and removed from the die

In experiment ABA5 a dry mix of 85 parts G-18 graphite flour and 15 parts TP-3 carbon black was compressed to 28,000 psi unloaded, and -- without removal from the die -- was compressed again to the same pressure unloaded and removed from the die Density under pressure for both cycles is plotted in Fig 5, for both

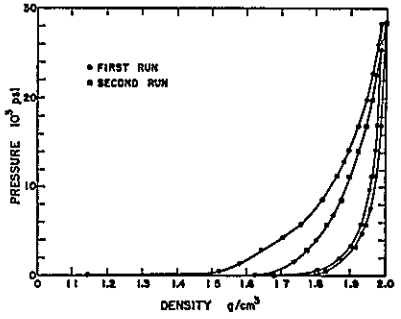

Fig 5 Pressure vs Bulk Density for Two Successive Cycles of Pressing a Dry Mix of 85 Parts G-18 Graphite Flour 15 Parts TP-3 Carbon Black

TABLE 11

DENSITIES OF DRY-PRESSED GRAPHITE FLOURS ALONE AND WITH CARBON-BLACK ADDITIONS

Specimen No	Composition: Flour	Fines	Densities: Particle	Packing	At Pressure: 28 KSI	566 PSI	15 PSI	Out of Die	Comments
	G-18	TP-3							
ABA5-1	85	15	2 15	1 64	1 987	1 805	1 625	---	1st cycle
					1 996	1 828	1 680	1 428	2nd cycle
	G-18	TP-3							
ABA6-1	85	15	2 15	1 64	1 989	1 808	1 607	1 394	in air - no vacuum
	G-25	TP-3							
ABA7-1	100	---	2 129	1 618	1 983	1 695	1 515	---	
ABA7-2	85	15	2 092	1 59	1 922	1 709	1 590	1 442	
ABA7-3	75	25	2 067	1 571	1 840	1 680	1 584	1 481	
ABA2-5	---	100	1 88	1 429	1 403	1 233	1 232	---	

TABLE 12

PERCENT OF PARTICLE DENSITY AND OF PACKING DENSITY ATTAINED IN DRY-PRESSING

Specimen No	Composition		% of Particle Density				% of Packing Density Based on Particle Density			
	Flour	Fines	28 KSI	566 PSI	14 PSI	Out of Die	28 KSI	566 PSI	14 PSI	Out of Die
	G-18	TP-3								
ABA5-1	85	15	92 4	84 0	75 6	---	121 2	110 1	99 1	---
			92 8	85 0	78 1	66 4	121 7	111 5	102 4	87 1
ABA6-1	85	15	92 5	84 1	74 7	64 8	121 3	110 2	98 0	85
	G-25	TP-3								
ABA7-1	100	---	93 1	79 6	71 2	---	122 6	104 8	93 6	---
-2	85	15	91 9	81 7	76 0	68 9	120 9	107 5	100	89 4
-3	75	25	89 0	81 3	76 6	71 6	117 1	106 9	100 8	94 3
-5	0	100	74 6	67 8	65 5	---	98 8	89 8	86 8	---

TABLE 13

SPRING BACK OF DRY PRESSED SPECIMENS

Specimen No	Composition		Spring Back of Specimens %			Comments
			28 KSI to 566 PSI	28 KSI to 14 PSI	28 KSI to atm	
	Flour	Fines				
	G-18	TP-3				
ABA5-1	85	15	8 4	16 8	---	cycle 1
			7 4	14 3	26	cycle 2
			7 8	14 7	26 4	cycle 2 based on density at 28 KSI in cycle 2
ABA6-1	85	13	8 4	17 8	27 7	
	G-25	TP-3				
ABA7-1	100	---	13 5	21 9	---	
-2	85	15	10 2	15 9	23	
-3	75	25	7 7	12 4	17 4	
ABA2-5	---	100	6 8	9 1	---	

loading and unloading Densities and spring-back are summarized in Tables 11, 12, and 13 Density at a given pressure is only slightly higher during the second cycle than during the first Any attempt to produce a high-density graphite by stress-relaxation in a binderless system will evidently require that the relaxation heat treatment be performed with the powder under high pressure rather than by cycling to high pressure at room temperature and then heat-treating under reduced pressure

To determine whether use of an evacuated die made any large difference in the experimental results, Run ABA6 was made in air, without evacuation of the die The data in Tables 11, 12 and 13 indicate no large difference between pressing in air and in an evacuated die Since the residual pressure in the evacuated die is normally greater than 1 mm air may still have an important lubricating role in the dry-pressing procedure used It is clear, however, that the high densities achieved under pressure do not result simply from evacuation of the system

The ABA7 series of experiments, also summarized in Tables 11, 12 and 13, was run to explore the dry-pressing behavior of a graphite flour having a blockier particle shape than that of G-18, which is somewhat acicular The flour used in the ABA7 series was from Lot G-25 a fine HCTE flour having a particle-size distribution similar to that of G-18 Bulk densities under pressure, percent of packing density attained and spring back during unloading were generally less than when G-18 flour was used, but the differences were much smaller than had been expected

E Effects of Binder Characteristics (J M Dickinson)

In the AAS series, the effects of viscosity and molecular distribution of furfuryl alcohol resin binders on manufacturing procedures and the properties of extruded graphites are being investigated The filler mix used throughout is 85 parts graphite flour (Lot G-18) and 15 parts carbon black ("regular" Thermax, Lot TP-3 or TP-4), with 27 pph of resin binder containing 4% maleic anhydride

The binders used so far have been commercial Varcum 5182 resin and the EW series of resins synthesized in CMF-13 Some of the CMF-13 resins used to make Lots AAS1 2, 4, 5, 7 and 9 were found to have increased in viscosity with time after their preparation and their viscosities at the times when the extrusions were made are not known Resins used to make subsequent lots of graphite were improved with regard to stability and their viscosities were measured both before and after the extrusion runs in which they were used Their properties, therefore, are known quite accurately

Extrusion conditions for the AAS graphites are summarized in Table 14 Using resins of widely different viscosity it is difficult to control extrusion pressures and speeds and variations in these parameters may be reflected in the properties of the graphites made

A large number of different curing cycles have been used for these graphites They are identified in Table 15 by the number of the cam used to program the heat treatment The cycle produced by each cam is described in Table 16 Initially the curing cycle extended only to 200°C, with holds at temperatures at which differential thermal analysis (DTA) had indicated thermal activity in the resin Cams 12 33, 34 35 and 36 produced such cycles and usually resulted in cracking either after baking or after graphitizing The fact that many specimens survived curing but cracked during baking, and the DTA evidence of a region of high thermal activity between 300° and 400°C led to use of a curing cycle extending to 420°C (Cams 42 43 44, 45 46 and 47) Use of a slow cure (2 5°C/hr) to 420°C seemed to minimize specimen damage for a wide range of resins and viscosities and will be the standard curing treatment for the rest of the AAS series In particular, the low heating rate reduced the incidence of rim cracks extending inward from the rod surface a few hundred microns and the high curing temperature minimized internal cracking

For properly-cured specimens the baking cycle appeared not to be critical That represented by Cam 16, involving moderately high heating rates to 900°C and a 2-hr hold at 900 C, has been used successfully

All specimens were graphitized in flowing helium in a cycle involving heating to 2800°C in 6 hr and furnace-

TABLE 14

BINDERS USED AND EXTRUSION CONDITIONS FOR AAS GRAPHITES

Lot No	Rod No	Binder		Extrusion Conditions			Green Dia, in
		Identification	Viscosity, cp	Temp, C	Pressure psi	Speed in /min	
AAS1	1 thru 8	EW-146	> 2200	50	7600	116	0 500
AAS2	1	EW-146	> 2200	52*	7600	92	0 500
AAS2	5 5B 6 6B	EW-146	> 2200	52	7600	116	0 500
AAS2	10 13,13B	EW-146	> 2200	60	7600	92	0 500
AAS2	9,9B 10B	EW-146	> 2200	60*	7600	116	0 500
AAS2	18	EW-146	> 2200	---	7600	116	0 500
AAS3	1 thru 14	Varcum 5182	250	52	6400	141	---
AAS4	1 thru 14	EW-146*	> 2200	60*	9500	82	0 501
AAS5	1 thru 14	EW-147	> 2600	54	8300	57	0 500
AAS6		Varcum 5182	250	50*	6400	112	0 505
AAS7		EW-147	> 2600	61	9500	116	0 500
AAS8	1 thru 9	Varcum 5182	250	52	7000	133	0 504
AAS8	10 thru 17	Varcum 5182	250	44*	7000	133	0 504
AAS8	18 19	Varcum 5182	250	<44*	7000	133	0 504
AAS9	1 thru 7	EW-153	> 2230	60*	10,200	78	0 500
AAS9	8 thru 14	EW-153	> 2230	60	10 200	54	0 500
AAS10	1 thru 18	EW-191	2770	54	11,800	61	0 500
AAS11	0 thru 7	EW-192	3909	60	14 000‡	100	0 4995
AAS11	8 thru 13	EW-192	3909	53	14,000‡	100	0 4995
AAS12	1 thru 9	EW-194	2457	55	13 400	110	0 500
AAS12	10 thru 16	EW-194	2457	45	13 400	110	0 500
AAS13	1 thru 18	EW-195	1300	50	9 500	120	0 502

* 26 5 ppb

‡ Dropping from 14 000 to 12 000 psi

TABLE 15

HEAT-TREATING CYCLES AND RESULTS, AAS GRAPHITES

Lot No	Rod No	Curing		Baking		Graphitized at 2800 C, Inspection
		Cam No	Inspection	Cam No	Inspection	
AAS1	1	33		38		Rim cracks
AAS1	1B	34		38		Rim cracks
AAS1	2	35		38		Rim cracks
AAS1	2B	36		38		Rim cracks
AAS1	5	33		37		Rim cracks
AAS1	5B	34		37		Rim cracks
AAS1	4	35		37		Rim cracks
AAS1	4B	36		37		Rim cracks
AAS1	6, 8	35		16		Rim cracks
AAS2	13	33		38		Rim cracks
AAS2	13B	34		38		Rim cracks
AAS2	10	35		38		Rim cracks
AAS2	10B	36		38		Rim cracks Central crack
AAS2	5	33		37		Rim cracks
AAS2	5B	34		37		Rim cracks
AAS2	6	35		37		Rim cracks
AAS2	6B	36		37		Rim cracks
AAS2	1, 9	33		16		Rim cracks
AAS2	9B	34		16		Rim cracks
AAS2	18	35		16		Rim cracks
AAS2	14B	36		16		Rim cracks Central crack
AAS3	1 thru 14	12		16		Some rim cracks, mostly OK
AAS4	6	34		38		OK
AAS4	7	36		38		OK
AAS4	5	12		38		OK
AAS4	3	34		37		OK
AAS4	4	36		37		OK
AAS4	1	12		37		OK
AAS4	9	34		16		OK
AAS4	10	36		16		OK
AAS4	8, 11, 14	12		16		OK
AAS5	7	34		38		OK
AAS5	8	36		38		OK
AAS5	9	12		38		OK
AAS5	6	12		37		OK
AAS5	4, 10	34		16		Cracked
AAS5	11	36		16		OK
AAS5	3, 12, 13 14	12		16		OK

TABLE 15 (Continued)

Lot No	Rod No	Curing		Baking		Graphitized at 2800°C
		Cam No	Inspection	Cam No	Inspection	Inspection
AAS6		12	OK	16	OK	OK
AAS7		12	OK	16	Cracked	Cracked
AAS8	1 6, 11, 16	42 to 200	1/4 cracked	16	1/4 cracked	1/2 cracked
AAS8	5 10 12	42 to 400	OK	16	OK	Fine side cracks
AAS8	2 7 12 17	41	OK	16	1/4 cracked	1/4 cracked
AAS8	3 8, 13 18	43	1/2 cracked	16	1/2 cracked	1/2 cracked
AAS8	4 9 14 19	44	OK	16	1/4 cracked	1/4 cracked
AAS9	1 6 11	42	2/3 cracked	16	2/3 cracked	All cracked
AAS9	2 7 10	41	OK	16	1/3 cracked	1/3 cracked
AAS9	3 8, 13	43	OK	16	OK	Cracked
AAS9	4 9 14	44	1/3 cracked	16	1/3 cracked	1/3 cracked
AAS9	5 12	12	OK	16	Cracked	Cracked
AAS10	1 5 9, 13	42	1/2 cracked	16	1/4 cracked	1/4 cracked
AAS10	2 6 10, 14	45	OK	16	OK	OK
AAS10	3, 7 11 15	46	1/2 cracked	16	1/4 cracked	1/4 cracked
AAS10	4 8 12 16	47	OK	16	1/4 cracked	1/4 cracked
AAS10	17 18	12	---	16	Cracked	Cracked
AAS11	1, 5, 9	42	Cracked	16	Cracked	Cracked
AAS11	2 6 10	45	Cracked	16	Cracked	Cracked
AAS11	3 7 11	46	Cracked	16	Cracked	Cracked
AAS11	4 8 12	47	1/3 cracked	16	1/3 cracked	All surface cracked
AAS11	0, 13	12	OK	16	Cracked	Cracked
AAS12	1, 6, 11, 16	42	OK	16	OK	3/4 cracked
AAS12	2, 7, 12	45	OK	16	OK	OK
AAS12	3 8 13	46	2/3 cracked	16	2/3 cracked	2/3 cracked
AAS12	4, 9, 14	47	2/3 cracked	16	2/3 cracked	2/3 cracked
AAS12	5, 10 15	12	OK	16	OK	2/3 cracked
AAS13	1 6, 11 16	42	OK	16	OK	OK
AAS13	2, 7, 12, 17	45	OK	16	OK	OK
AAS13	3 8, 13, 18	46	OK	16	OK	OK
AAS13	4 9, 14 3rd	47	OK	16	OK	OK
AAS13	5, 10 15 2nd	12	OK	16	OK	OK

TABLE 16

CAM-CONTROLLED HEAT-TREATING CYCLES

Cam # 12 -- a 72 hr cycle
- 20 to 45°C at 3 125 °/hr
- hold 10 hr at 45 C
- 45 to 90 C at 5°/hr
- 90 to 138 C at 2°/hr
- 138 to 200°C at 5 167 /hr
- hold 8 hr at 200 C
- Furnace Cool to Room Temperature

Cam # 33 a + b -- a 144 hr cycle
- 20 to 50°C at 2 5°/hr
- 50 to 200 C at 1 136 /hr
- Furnace Cool to Room Temperature

Cam # 34 a + b -- a 144 hr cycle
- 20 to 90 C at 2 5°/hr
- hold 40 hr at 90 C
- 90 to 140 C at 2 5°/hr
- hold 140 C for 32 hr
- 140 to 200 C at 2 5 /hr
- Furnace Cool to Room Temperature

Cam # 35 -- a 72 hr cycle
- 20 to 200°C at 2 5 /hr
- Furnace Cool to Room Temperature

Cam # 36 -- a 72 hr cycle
- 20 to 90°C at 5 /hr
- hold 20 hr at 90°C
- 90 to 140°C at 5°/hr
- hold 16 hr at 140 C
- 140 to 200°C at 5 /hr
- Furnace Cool to Room Temperature

Cam # 16 -- a 44 hr cycle
- 20 to 450°C at 19 545°/hr
- 450 to 900 C at 23 682°/hr
- hold 2 hr at 900°C
- Furnace Cool to Room Temperature

Cam # 37 -- a 63 hr cycle
- 20 to 55°C at 0 769°/hr
- 55 to 310°C at 13 42 /hr
- hold 16 hr at 310°C
- 310 to 400°C at 22 5 /hr
- 400 to 900 C at 33 333°/hr
- Furnace Cool to Room Temperature

Cam # 38 -- a 60 hr cycle
- 20 to 825°C at 13 417°/hr
- Furnace Cool to Room Temperature

Cam # 42 -- a 40 hr cycle
- 20 to 420 C at 10°/hr
- Furnace Cool to Room Temperature

Cam # 43 -- a 72 hr cycle
- 20 to 425°C at 5 5 /hr
- Furnace Cool to Room Temperature

Cam # 44 -- a 71 hr cycle
- 20 to 100°C at 12 5°/hr
- 100 to 185 C at 2 /hr
- 185 to 425 C at 10 7°/hr
- Furnace Cool to Room Temperature

Cam # 45 -- a 53 5 hr cycle
- 20 to 420°C at 7 5°/hr
- Furnace Cool to Room Temperature

Cam # 46 -- a 80 hr cycle
- 20 to 420°C at 5 /hr
- Furnace Cool to Room Temperature

Cam # 47 -- a 160 hr cycle
- 20 to 420°C at 2 5°/hr
- Furnace Cool to Room Temperature

cooling to essentially room temperature in about 3 hr

Properties so far determined on the graphitized specimens are listed in Table 17

Plots both of graphitized density (Fig 6) and of green rod diameter (Fig 7) vs extrusion pressure show rather abrupt changes in slope between 8000 and 10,000 psi Evidently, with the extrusion equipment and materials being used, there is little further compaction when pressure is increased above about 10 000 psi

As is illustrated in Fig 8, the extrusion pressure required increases rapidly with viscosity of the binder resin Scatter is broad due perhaps to lubricating effects of certain binders and to temperature variations in the mix and

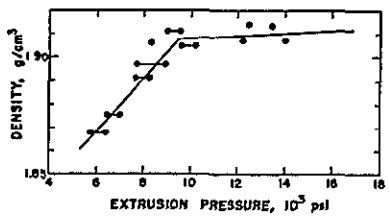

Fig 6 The Effect of Extrusion Pressure on Density AAS Graphites

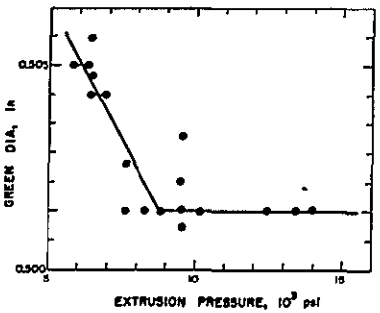

Fig 7 The Effect of Extrusion Pressure on Diameter of the Green Extruded Rod AAS Graphites

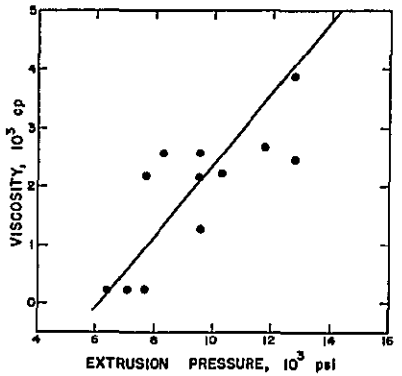

Fig 8 The Effect of Binder Viscosity on Extrusion Pressure, AAS Graphites

the die, but the relation is roughly linear The rapid increase of pressure with viscosity indicates why with a fixed binder to filler ratio and wide variations in binder viscosity it was impossible to maintain constant extrusion conditions throughout the series

The effects of binder viscosity on binder carbon residue and graphitized density are illustrated in Fig 9 and 10 Increasing viscosity above about 2000 cp had little effect on either The increase in carbon residue with binder viscosity accounts for only about one-half of the

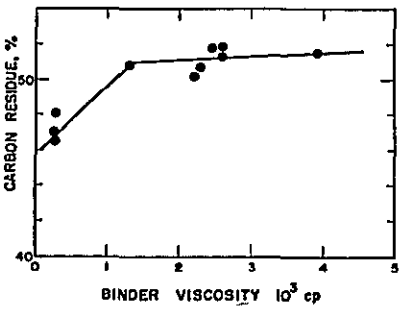

Fig 9 The Effect of Binder Viscosity on Binder Carbon Residue, AAS Graphites

TABLE 17

PROPERTIES OF AAS GRAPHITES

Lot No	Rod No	Carbon Residue, %	Density, g/cm³	Electrical Resistivity, μΩcm	Young's Modulus 10⁶ psi
AAS1	1	45-46	1 865	1044	
AAS1	1B	45-46	1 879	1101	
AAS1	2	45-46	1 886	1101	
AAS1	2B	45-46	1 879	1059	
AAS1	5	45-46	1 878	950	
AAS1	5B	45-46	1 885	---	
AAS1	4	45-46	1 884	951	
AAS1	4B	45-46	1 883	951	
AAS1	6,8	45-46	1 892	1112	
AAS2	13	44-45	1 887	1047	
AAS2	13B	44-45	1 890	1042	
AAS2	10	44-45	1 898	1047	
AAS2	10B	44-45	1 892	1042	
AAS2	5	44-45	1 884	936	
AAS2	5B	44-45	1 893	936	
AAS2	6	44-45	1 896	936	
AAS2	6B	44-45	1 890	945	
AAS2	1,9	44-45	1 880	1050	
AAS2	9B	44-45	1 890	945	
AAS2	18	44-45	1 897	1042	
AAS2	14B	44-45	1 891	1031	
AAS3	1 thru 14	---	1 868	1092	
AAS4	6	---	1 906	1069	
AAS4	7	---	1 906	941	
AAS4	5	---	1 900	993	
AAS4	3	---	1 899	1079	
AAS4	4	---	1 897	985	
AAS4	1	50 1	1 902	1072	
AAS4	9	---	1 907	948	
AAS4	10	---	1 909	975	
AAS4	8, 11, 14	49 9	1 906	1037	
AAS5	7		1 907	928	
AAS5	8		1 905	955	
AAS5	9		1 902	985	
AAS5	6		1 906	912	
AAS5	4, 10		1 905	993	
AAS5	11		1 906	983	
AAS5	3, 12 13, 14		1 905	1058	

TABLE 17 (Continued)

Lot No	Rod No	Carbon Residue %	Density, g/cm^3	Electrical Resistivity, μΩcm	Young's Modulus, 10^6 psi
AAS6			1 868	1147	
AAS7			1 911	1172	
AAS8	1, 6 11 16		1 884		
AAS8	5 10 12		1 871		
AAS8	2 7, 12 17		1 877		
AAS8	3 8 13, 18		1 876		
AAS8	4 9 14 19		1 876		
AAS9	1, 6, 11		1 901	1115	
AAS9	3 7, 10		1 906	1108	
AAS9	3 8 13		1 907	1110	
AAS9	4 9, 14		1 905	1105	
AAS9	5 12		1 906	1099	
AAS10	1, 5 9, 13	49 8±0 2	1 906±0 003	1053±60	2 68±0 1
AAS10	2 6 10 14	50 2±0 3	1 910±0 003	1051±89	2 69±0 1
AAS10	3 7 11 15	50 2±0 1	1 912±0 003	1078±30	2 71±0 1
AAS10	4 8, 12 16	50 9±0 1	1 914±0 001	1015±84	2 71±0 04
AAS10	17, 18	51 4±0 3	1 908±0 003	1020±20	2 71±0 02
AAS11	1 5 9	50 7±0 2	1 903±0 001	1030±41	2 61±0 06
AAS11	2 6 10	51 2±0 2	1 902±0 003	1029±43	2 63±0 04
AAS11	3 7, 11	51 3±0 1	1 907±0 003	1039±26	2 65±0 02
AAS11	4 8, 12	51 6±0 1	1 908±0 005	1001±69	2 65±0 05
AAS11	0 13	51 6±0 1	1 898±0 004	1056±25	2 58±0 14
AAS12	1 6 11 16	51 3±0 2	1 911±0 005	1058±13	2 63±0 06
AAS12	2 7 12	51 0±0 1	1 912±0 004	1031±25	2 63±0 06
AAS12	3 8, 13	51 0±0 3	1 911±0 004	1016±42	2 65±0 04
AAS12	4 9 14	50 9±0 2	1 913±0 001	1039±43	2 68±0 02
AAS12	5, 10, 15	51 7±0 1	1 907±0 002	1038±20	2 6±0 04
AAS13	1 6 11 16	50 1±0 4	1 901±0 002	984±8	2 62±0 02
AAS13	2 7, 12 17	50 2±0 3	1 904±0 001	982±14	2 65±0 03
AAS13	3, 8, 13, 18	50 4±0 2	1 905±0 003	976±21	2 65±0 04
AAS13	4 9 14 3rd	50 8±0 4	1 904±0 002	979±23	2 64±0 01
AAS13	5, 10, 15, 2nd	50 9±0 05	1 908±0 0005	969±19	2 69±0 01

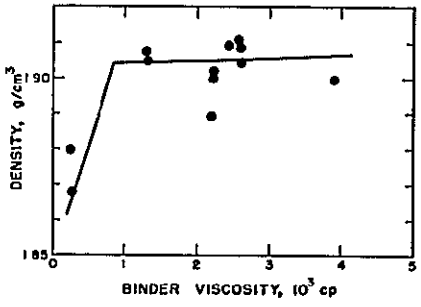

Fig 10 The Effect of Binder Viscosity on Graphitized Density, AAS Graphites

accompanying increase in density The rest of the density change must be attributed to the resulting increase in extrusion pressure, which reduced diameter of the green extruded rod and finally increased graphitized density

Young's modulus and electrical resistivity of the finished graphite were not much affected by variations in viscosity extrusion pressure and heat-treating cycles preceding graphitization

F Boronated Graphites, AAM Series (J M Dickinson)

The AAM series of boronated graphites has been made primarily for use in thermophysical-properties studies Compositions and extrusion conditions are summarized in Table 18 in which two similar, boron-free graphites from the AAP series have been included for the purpose of estimating batch-to-batch variations of properties of nearly identical graphites All graphites listed were cured and baked in similar cycles Lots AAM3 and AAM4 were graphitized only to 2400 C All other lots were graphitized to 2800 C Preliminary results from properties measurements indicate that the boron-containing graphites are remarkably uniform in properties, and that even very small boron additions have large effects on thermal and electrical properties

V STRUCTURAL STUDIES

A X-Ray Diffraction (J A O'Rourke)

1 Characterization of Coke Flours

Four of the commercial coke flours used as fillers in manufacture of the 34 Series of hot-molded graphites described above have been examined by x-ray diffraction in the as-received condition and after 30-min heat treatments at 2000°C and 3100°C Flours C-3, C-4 and C-5

TABLE 18

MIX COMPOSITIONS AND EXTRUSION CONDITIONS, AAM GRAPHITES

Lot No	Mix Composition, % G-18 Graphite Flour	Thermax Carbon Black	Boron Metallic Powder	Varcum 5182 Binder	Extrusion Conditions Pressure, psi	Speed, in /min	Dia Green Rod, in
AAM4	66 93	11 81 (TP-3)	0	21 26	6400	144	0 505
AAP29	66 93	11 81 (TP-3)	0	21 26	6400	150	0 504
AAP30	66 93	11 81 (TP-4)	0	21 26	7600	171	0 502
AAM6	66 88	11 81 (TP-4)	0 041	21 24	5700	171	0 504
AAM7	66 85	11 81 (TP-4)	0 081	21 26	5700	171	0 504
AAM8	66 77	11 81 (TP-4)	0 158	21 26	5700	171	0 505
AAM3	66 37	11 59 (TP-3)	0 79	21 26	6400	144	0 505

TABLE 19

CRYSTALLINE PARAMETERS OF COKE FILLER FLOURS

Lot No	Heat Treatment	Component	L_c Å	d_{002}, Å
C-3	None	Crystalline	800	3 36
C-3	None	"Amorphous	23 7	3 44
C-3	30 min at 2000 C	Composite	340	3 375
C-3	30 min at 3100°C	Composite	410	3 367
C-4	None	Crystalline	>1000	3 36
C-4	None	"Amorphous	24 6	3 44
C-4	30 min at 2000 C	Composite	259	3 391
C-4	30 min at 3100°C	Composite	290	3 368
C-5	None	Crystalline	>1000	3 36
C-5	None	"Amorphous	24 5	3 44
C-5	30 min at 2000 C	Composite	257	3 389
C-5	30 min at 3100 C	Composite	320	3 368
C-10	None	---	29 2	3 44
C-10	30 min at 2000 C	---	330	3 387
C-10	30 min at 3100°C	---	495	3 364

were Gilsocarbons nominally 100-mesh, 200-mesh and 325-mesh respectively Flour C-10 was Great Lakes Grade 3607 coke flour, which was relatively coarse and was ground to -100 mesh for x-ray examination After grinding it was no longer isotropic in behavior but packed in the x-ray sample holders with a fairly high degree of planar anisotropy

In the as-received condition, all three of the Gilsocarbons contained two distinct components, one of which was crystalline and the other nearly amorphous The coarsest flour, Lot C-3 had nearly 50% of the crystalline component, and the other two had much smaller amounts In Table 19, crystalline parameters are listed for both components of the as-received Gilsocarbons After heat-treatment at 2000°C the diffraction profiles from all three of these materials continued to demonstrate the presence of the two components, but the peaks could no longer be resolved for separate analysis and only average parameters are listed After heat-treatment at 3100°C only a slight indication of the second component could be detected The material was quite highly crystalline, although on the average less so than the very highly crystalline component present in the as-received material

Lot C-10 appeared to be a normal coke, which graphitized quite well However, the degree of crystallinity attained in heat-treatment at 2000°C was unexpectedly high

2 Crystalline Parameters and Anisotropies of Commercial Graphites

Four samples of commercial graphite were examined for LASL Group CMF-9 to determine their crystalline parameters and anisotropies, as an aid to explanation of properties differences thought to exist among them The x-ray results are listed in Table 20 The LASL sample of AGOT graphite was received in the form of a cylindrical shape which had been machined with its cylinder axis approximately normal to the extrusion axis It was not possible to locate the extrusion axis accurately enough to determine the variation in basal-plane concentration at low values of the angle Φ In this case therefore, anisotropy is characterized by the M-value only

TABLE 20

CRYSTALLINE PARAMETERS AND ANISOTROPIES OF COMMERCIAL GRAPHITE SAMPLES

Grade	L_c (Å)	d_{002} (Å)	M	σ_{ox}/σ_{oz}
AGOT (LASL)	510	3 361	2 5	---
AGOT (Battelle)	525	3 360	2 86	1 61
CCH	565	3 361	3 6	1 94
CEQ	116	3 404	~0 20	<1 05

The AGOT samples from LASL and from Battelle differed very little in crystalline parameters and anisotropy Grade CCH was similar to AGOT in degree of crystallinity but had a distinctly higher degree of preferred orientation Unlike the other two grades, CEQ is a molded rather than an extruded graphite The sample examined was nearly isotropic and was not highly graphitic

3 Pyrocarbons and Pyrographites

Crystalline parameters have been determined and impurity studies made on a variety of pyrolytic carbons and graphites in various conditions of heat treatment, for LASL Group CMB-8 Results of these examinations will be reported by CMB-8

B Optical and Electron Microscopy (R D Reiswig, L S Levinson)

1 Heat-Treated Carbon Black

It was previously reported (in LA-3932-MS) that a small sample of Thermax carbon black had been heat-treated for 30 min at 2800°C and observed to change in particle shape from spherical to polyhedral and to graphitize extensively The changes were unexpectedly large, and the possibility was considered that some catalyzing impurity had been present in the crucible used The experiment was therefore repeated on another sample from the same lot (TP-5) of carbon black, using a clean crucible which had itself been heat-treated to 2830°C The same changes in the carbon black were observed to occur to about the same degree, and it is concluded that this is the normal behavior of Thermax carbon black

2 Fracture Path in AAQ1 Graphite

Longitudinal sections through several AAQ1 graphite test bars which had been broken in tension at a variety of temperatures have been examined, primarily to observe the path followed by the fracture Attempts to do so by mounting and sectioning only one half of the test bar were unsuccessful principally because, whether a filler grain or binder residue was exposed locally at the fracture surface it was never known whether the matching region in the opposite surface represented the same mix component or an interface with the other component Accordingly one half of one test bar was electroplated with silver to a thickness of about 0 000,1 in the bar was reassembled and sectioned and the section was examined microscopically With the silver present to mark the fracture path positively, optical microscopy at low magnification was reasonably satisfactory However the metallic layer was too thick and mating of opposing surfaces too imprecise for electron microscopy Best results were obtained by simply reassembling the broken specimen with no preparation of its fracture surfaces mounting the reassembled specimen in a low-viscosity epoxy mounting resin and depending on vacuum-impregnation during mounting to mark the fracture path and associated crack system with resin It did so very effectively

In AAQ1 graphite broken in tension at room temperature or at any elevated temperature to 2750°C, the frac-

ture path is partly through filler particles, partly through binder residue and partly along filler-binder interfaces Unlike high-density pitch-bonded materials, where transgranular facture is in general quite strongly preferred, the fracture path in this resin-bonded graphite showed some preference for the binder residue However, where the fracture encountered a filler particle whose lamellar internal structure was approximately normal to the tension axis then the filler particle was cleaved Where the lamellae of the filler grain were nearly parallel to the tension axis the fracture path usually detoured the grain following its interface with the binder

3 Scaly vs Lamellar Microstructures

As has been described in previous reports in this series, the internal structure of a reasonably well-crystallized graphite may have either a scaly or a lamellar appearance according to the orientation of the basal planes in the graphite relative to the section examined The transition from one appearance to the other has been observed to occur very sharply as this angle was changed but the precise angle at which the transition occurred could not be determined because of ambiguities in measuring the orientations of non-planar graphite layers

In an attempt to determine this transition angle more precisely sections were examined which had been cut at various angles through a specimen of pyrolytic graphite whose structure had been improved by a high-temperature swivelling treatment. Locally the graphite layers were essentially flat, and good angular measurements were possible It was found that when the angle between the surface examined and the average basal plane orientation was 45° or less, the graphite structure appeared scaly When this angle was 48 or more, it appeared lamellar At angles between 45 and 48° the appearance was a mixture of scaly and lamellar patterns

4 Tested Creep Specimens

Three specimens of AAQ1 graphite which had been tested in tensile creep were examined microscopically particularly to determine the nature and thickness of vapor-deposited coatings produced presumably by vaporization of carbon from the graphite heater tube and its condensation on the slightly cooler specimen A specimen tested at 2500 C showed no detectable deposit One tested at 2650°C had a coating ranging in thickness up to 10μ, whose internal structure had the appearance of a pyrolytic graphite The third specimen, tested at 2720 C until the heater tube burned out, had a similar coating up to 100μ thick, some of which may have been deposited when heater burnout occurred

In previous experiments, similar coatings on tensile test bars have been found to have no significant effect on ultimate tensile strength subsequently measured at room temperature It is not clear, however, that their effect is equally small when the test is made at the temperature at which the coating was deposited, or that it is the same in a creep test as in a tensile test made at a much higher strain rate The possibility remains then, that the thicker deposits produced in tests made above about 2500 C may significantly affect the creep behavior observed

VI PHYSICAL AND MECHANICAL PROPERTIES

A Sound-Velocity Studies (P E Armstrong)

A series of measurements has been made on a group of hot-molded pitch-bonded graphite specimens made from the products of grinding commercial Grade YBF graphite in a fluid-energy mill The specimens, listed in Table 21, were in the form of rectangular parallelepipeds 0 5 x 0 5 x 2 0 in , machined from 2 5-in dia molded discs Thin-rod resonance frequencies and 3MHz pulse-transmission velocities were determined and compared with thin-rod measurements previously made on 0 25-in dia rods machined from the same discs The 3MHz pulse was essentially absorbed by specimens S-4-3 S-5-3 and S-6-3, made from the coarser fillers so that no detectable signal reached the receiving transducer

The "thin-rod" resonance measurements on the rectangular specimens produced Young's modulus values which were within 4% of previous thin-rod measurements on 0 25-in dia rods

TABLE 21

SOUND-VELOCITY MEASUREMENTS ON HOT-MOLDED, PITCH-BONDED GRAPHITES SERIES S

Specimen No	Filler Used Lot No	% <5μ	0 25-in dia Thin Rod Density, g/cm³	0 25-in dia Thin Rod Young's Modulus * 10⁶ psi	Rectangular Parallelepiped Density, g/cm³	Rectangular Parallelepiped Young's Modulus * 10⁶ psi	Rectangular Parallelepiped "Thin-Rod" Velocity * 10⁵ in /sec	Rectangular Parallelepiped Bulk Velocity 10⁵ in /sec
S-2A-3	T(YBF)-12	99 1	1 863	2 998	---	---	---	---
			1 862	3 004	1 861	3 212	1 36	1 31*
			---	---	---	---	---	1 00‡
S-3-3	T(YBF)-4	43 3	1 876	2 752	---	---	---	---
			1 872	2 765	1 866	2 739	1 25	1 31*
			---	---	---	---	---	0 61‡
S-4-3	T(YBF)-2	16 7	1 832	1 807	---	---	---	---
			1 827	1 746	1 891	1 866	---	---
S-5-3	T(YBF)-1	10 4	1 820	1 484	---	---	---	---
			1 843	1 502	1 840	1 536	---	---
S-6-3	GP(YBF)-6	2 6	1 788	1 140	---	---	---	---
			1 793	1 021	1 783	1 134	---	---

* With-grain

‡ Across-grain

Bulk velocities from pulse-transmission measurements in theory cannot be compared directly to thin-rod velocities, although in this case the values differ by only about 5% The ratio of bulk velocities perpendicular and parallel to the pressing direction yields one kind of anisotropy ratio This was 1 31 for specimen S-2A-3 made from the finest filler, and 2 15 for specimen S-3-3, made from the next coarser flour The squares of these ratios, 1 72 and 4 62 should approximate the anisotropy ratios with regard to Young's moduli There is no obvious correlation between these two sets of anisotropy ratios and ratios for the same graphites based on electrical resistivity, thermal expansion or crystallographic orientation, except that all of them indicate a relatively high degree of anisotropy in both samples In properties other than bulk velocity and Young's modulus, it is the graphite made from the finest flour which is most anisotropic

B Static vs Dynamic Young's Moduli (P E. Armstrong)

On the basis of previous experiments here and elsewhere in general involving pitch-bonded commercial graphites it has been assumed that the value of Young s modulus determined dynamically (e g by a resonance technique) is the same as that which would be determined statically (e g in a low strain-rate tensile test) at very low loads or after a few cycles of loading and unloading Dynamic Young's modulus has therefore been used generally in this series of reports without comment

Recent experiments on AAQ1 graphite described in detail in a topical report on that material now being prepared, suggest that this assumption may not be correct

at least for resin-bonded graphites The dynamic measurements involved were very reproducible and are reported with confidence For consistency all static measurements were made in low strain-rate tensile tests during initial loading of previously unstrained specimens, and using an optical tracking system for strain measurements For several reasons the quality of the static measurements was not high However, for temperatures below about 1500°C they appeared to indicate a static modulus which initially was considerably below the dynamic modulus although it increased somewhat on repeated loading Above 1500 C the initial static modulus appeared to decrease quite rapidly with increasing temperature while the dynamic modulus continued to increase toward a maximum value near 2300 C

In a preliminary exploration of the relation between static and dynamic values of Young's modulus in resin-bonded graphites both types of measurements were made at room temperature on three specimens of AAQ1 graphite having gage sections 0 25-in dia and 9 in long Dynamic measurements were made by a thin-rod resonance technique which gave values of $2\ 375 \times 10^6$ $2\ 37_5 \times 10^6$ and $2\ 386 \times 10^6$ psi for the individual rods Static measurements were made in a low-level stress-strain apparatus in which slowly-applied dead-weight loading is used to develop tensile stress up to about 22 psi and strain is measured with an unbonded strain gage In spite of precise instrumentation, careful measurements and use of a very low stress range static modulus values scattered broadly and erratically from specimen to specimen and during successive cycles of loading and unloading the same specimen Most probably values were judged to be $2\ 12 \times 10^6$, $2\ 25 \times 10^6$ and $2\ 01 \times 10^6$ psi Load vs extension records were generally curved during the first cycle or two of loading their slope decreasing with increasing strain becoming essentially linear in later cycles Usually but not always a lower loading rate (4 5 psi/min) gave lower and less consistent modulus values than did a higher rate (0 0 psi/min) Modulus measured during loading was usually, but not always lower than that measured during subsequent unloading

Static Young's moduli determined in this way were significantly lower than the dynamic moduli of the same specimens although distinctly higher than those derived from the regular tensile tests In view of the anelastic behavior of graphite it is possible that -- even at room temperature -- this indicates a time-dependent relaxation which reduces the apparent modulus in a "static' test Unless and until this is demonstrated, however it is simpler to assume that for this type of graphite, at least the stress-strain curve is quite strongly curved even at very low stresses

C Torsional Properties (D T Eash)

Sixteen specimens of commercial Grade AUC graphite have been tested in torsion at room temperature in a recently-completed torsional adapter for an Instron mechanical tester Average modulus of rupture was 1985 psi with standard deviation of 185 psi Additional tests are planned on the same material to investigate the usefulness in this application of a quick-setting epoxy cement, to attach specimen ends to loading fixtures If this cement is satisfactory its use will greatly reduce the time required for sample preparation

D Creep Properties and Mechanisms (W V Green, E G Zukas, J Weertman)

1 AAQ1 Graphite

Primarily to compare the operation and results of a new creep-testing furnace with those of the unit previously used, several additional tensile creep tests have been made on AAQ1 graphite Two tests at 2500 C and 5260 psi gave results which agreed well with those previously reported for the same temperature and stress A change-in-load test made at 2720°C indicated that creep rate was proportional to the 6 9 power of stress, compared with previously-reported values of 7 8 at 2500°C and 9 2 at 2300°C A change-in-temperature test over the range 2400° to 2650°C gave an apparent activation energy for tensile creep of 232 kcal/mole, compared with about 250 kcal/mole previously reported

These results are felt to represent good agreement with those obtained on the same graphite in the system previously used

2 Fracture-Mechanics Studies

An attempt is being made to apply the techniques of fracture mechanics to the problem of creep in graphite The equations used in fracture mechanics have been modified to include consideration of time-dependent creep strain in a highly anisotropic system At least mathematically the picture that is being developed resembles certain dislocation models of crack extension and opening in more conventional materials

Experimentally, tensile bars of the same design as those previously used for sequential microscopy have been machined from ZTA graphite, with the tensile axis parallel to the preferred c-axis direction so that large strains will precede fracture Under creep conditions, a hole drilled through the center of the gauge section has been observed to grow by spreading of cracks normal to the tension axis outward from the edges of the hole At first the creep strain is so localized that it does not measurably increase the gage length of the specimen However, local strain can be measured at this stage by interrupting the creep tests at intervals and photographing the same areas on the specimens repeatedly at moderately high magnification Subsequently, as creep is continued, the zone in which cracks develop spreads throughout the specimen and the increase in gage length becomes easily measurable

E Thermal Conductivity (P Wagner)

Samples of AAQ1 graphite have been furnished to LASL Group N-1 for their independent measurements of its thermal conductivity This lot of graphite is uniform enough and sufficiently well characterized so that it may prove to be useful as a reference material for high-temperature conductivity measurements

Thermal conductivities of specimens of Armco Iron, molybdenum, and tungsten, which will be used by LASL Group CMB-11 as reference materials in a series-comparison conductivity apparatus, were determined by the flash-diffusivity technique

F Thermal Expansion (P Wagner, P E Armstrong)

In collaboration with other NERVA-ROVER Laboratories, CMF-13 is participating in a "round-robin" series of high-temperature thermal-expansion measurements on a sample of POCO Grade AMX-5Q graphite Two independent sets of measurements will be made in CMF-13 which will be compared with the results of measurements by other laboratories

END

DATE FILMED

12 / 23 / 68